The Astrophysical Journal Letters, 906:L5 (10pp), 2021 January 1 https://doi.org/10.3847/2041-8213/abcec9

On the True Fractions of Repeating and Nonrepeating Fast Radio Burst Sources

Shunke Ai[1], He Gao[2], and Bing Zhang[1]
[1] Department of Physics and Astronomy, University of Nevada Las Vegas, Las Vegas, NV 89154, USA; ais1@unlv.nevada.edu, zhang@physics.unlv.edu
[2] Department of Astronomy, Beijing Normal University, Beijing 100875, People's Republic of China; gaohe@bnu.edu.cn
Received 2020 July 5; revised 2020 November 20; accepted 2020 November 30; published 2021 January 6

Abstract

Observationally, fast radio bursts (FRBs) can be divided into repeating and apparently nonrepeating (one-off) ones. It is unclear whether all FRBs repeat and whether there are genuine nonrepeating FRBs. We attempt to address these questions using Monte Carlo simulations. We define a parameter T_c at which the accumulated number of nonrepeating sources becomes comparable to the total number of repeating sources, which is a good proxy to denote the intrinsic repeater fraction among FRBs. Assuming that both types of sources exist and their burst energies follow power-law distributions, we investigate how the observed repeater fraction evolves with time for different parameters. If the lifetime of repeaters is sufficiently long that the evolutionary effect can be neglected within the observational time span, unless $T_c \to \infty$ (i.e., there is no genuine nonrepeating FRB source), the observed repeater fraction should increase with time first, reach a peak, and then decline. The peak time T_p and peak fraction $F_{\rm r,obs,p}$ depend on T_c and other repeating rate parameters. With the current data, we pose a lower limit $T_c > 0.1$ day for reasonable parameter values. We predict that future continuous monitoring of FRBs with CHIME or similar wide-field radio telescopes would obtain an $F_{\rm r,obs}$ less than 0.04. The detection of a smaller peak value $F_{\rm r,obs,p} < 0.04$ in the near future would disfavor the ansatz that "all FRB sources repeat."

Unified Astronomy Thesaurus concepts: Radio transient sources (2008)

1. Introduction

Fast radio bursts (FRBs) are mysterious transients originating from a distant point in the universe (Lorimer et al. 2007; Thornton et al. 2013; Cordes & Chatterjee 2019; Petroff et al. 2019). Even though early observations only detected one-off events, the discovery of multiple bursts from FRB 121102 (Spitler et al. 2016) suggested that at least some are repeating sources. Recent observations by CHIME revealed that repeating FRBs are commonly observed (CHIME/FRB Collaboration et al. 2019a, 2019b).

One intriguing question is whether there exist genuinely nonrepeating FRBs. The difficulty in addressing this problem lies in the wide range of repeating waiting times (Palaniswamy et al. 2018; Caleb et al. 2019) and FRB luminosities (Luo et al. 2018, 2020; Lu & Piro 2019). It is highly likely that some apparently nonrepeating FRBs are actually repeaters. The nondetection of the repeated bursts could be because of the long waiting time or low flux of the repeating bursts (Palaniswamy et al. 2018). The high event rate of FRBs may suggest that the majority of FRBs are repeaters (Ravi 2019). On the other hand, deep follow-up observations of some FRBs (e.g., the famous "Lorimer" event) did not reveal repeated bursts (Petroff et al. 2015). Palaniswamy et al. (2018) and Caleb et al. (2019) argued that active repeaters such as FRB 121102 are abnormally active. If all FRBs are similar to FRB 121102, many one-off bursts should have been detected as repeaters.

However, repeating FRBs may have different repetition levels. If FRBs have a wide range of repetition rates, it is possible that the ansatz "all FRB sources repeat" is true (e.g., Lu et al. 2020). Are there indeed genuine nonrepeaters? If so, how can we find out that they exist? What are the true fractions of repeaters and nonrepeaters?

In this letter, we attempt to address these questions through Monte Carlo simulations. The basic formalism of our approach is described in Section 2. The simulation methodology is outlined in Section 3, and the results are presented in Section 4. Section 5 presents conclusions with some discussion.

2. Basic Formalism

A repeating FRB source can produce a sequence of bursts, but only those with energy exceeding a threshold value are detectable. Below, we follow Lu et al. (2020) to calculate the repeating rate of repeaters but add a population of genuine nonrepeaters. We assume that the threshold fluence for a detector to trigger an FRB event is $F_{\rm th}$. For a source at the luminosity distance D_L, the threshold energy for a burst to be detectable is

$$E_{\rm th} = 4\pi D_L^2 F_{\rm th}(1+z)^{\alpha-1}, \tag{1}$$

where a k-correction has been introduced and α is the intrinsic spectral index of the burst ($S_\nu \propto \nu^{-\alpha}$), with $\alpha = 1.5$ adopted.

Consider that the repeating rate of a repeating FRB source is related to the intrinsic energies of the bursts as a power-law function, i.e.,

$$\frac{dr}{dE} = \frac{r_0}{E_0}\left(\frac{E}{E_0}\right)^{-\gamma}\exp\left(-\frac{E}{E_{\rm max}}\right), \tag{2}$$

where $\gamma = 1.92$ is inferred from the current repeating FRB sample (Lu et al. 2020). We set $E_0 = 10^{30}$ and $E_{\rm max} = 10^{34}$ erg Hz^{-1} (Lu & Piro 2019). Here r_0 is a normalization parameter, which stands for the intrinsic repeating rate of the bursts at $E = E_0$. For FRB 121102, the measured value is $r_0 = 0.1$ hr^{-1} (Law et al. 2017; James 2019). Then, the effective repeating rate of bursts above $E_{\rm th}$ could be calculated as

$$r(>E_{\rm th}) = r_0 \int_{x_{\rm th}}^{\infty} dx x^{-\gamma}\exp\left(\frac{-xE_0}{E_{\rm max}}\right), \tag{3}$$

where $x = E/E_0$ and $x_{\rm th} = E_{\rm th}/E_0$. In view of the detection of the Galactic FRB 200428 (Bochenek et al. 2020; the CHIME/FRB Collaboration et al. 2020), we also introduce a low-energy cutoff energy at $E_{\rm min} = 10^{28}$ erg Hz^{-1}.

As a function of r, the distribution of time intervals (δ) between two adjacent bursts could be described by a Weibull probability density function (Oppermann et al. 2018), which reads

$$\mathcal{W}(\delta|k, r) = k\delta^{-1}[\delta r\Gamma(1 + 1/k)]^k e^{-[\delta r\Gamma(1+1/k)]^k}, \quad (4)$$

where k is the shape parameter. When $k = 1$, the time interval distribution reduces to the exponential distribution; when $k < 1$, the bursts are clustered; and when $k > 1$, the bursts tend to be periodic. A detailed discussion of the time interval distribution is shown in the Appendix.

For nonrepeating FRBs to be detectable, they should also exceed the threshold energy shown in Equation (1). Assume that the energy of nonrepeating FRBs follows a simple power-low distribution as

$$\frac{dN}{dE} \propto E^{-\gamma_n}, \quad (5)$$

with $E_{\rm n,min} < E < E_{\rm n,max}$, and we take $E_{\rm n,min} = 10^{30}$ erg Hz^{-1}, $E_{\rm n,max} = 10^{34}$ erg Hz^{-1}, and $\gamma_n = 1.8$ (Lu & Piro 2019; Luo et al. 2020).[3]

2.1. Nonevolving Repeaters

In a steady state, the birth and death rates of the repeating sources would balance each other, so that the total number of sources in the sky would be a constant. Assuming that the lifetimes of the repeaters are much longer than the observational timescale and that the bursts from each source are produced with a constant repeating rate, one can approximately regard that the repeaters are not evolving. The intrinsic repeating rate for each individual repeater may not be the same but rather follow a certain distribution. In this subsection, we deal with this case and defer the evolving case to the next subsection.

For genuine nonrepeating sources, the progenitor of the FRB produces an FRB once in its lifetime. The number of nonrepeating sources accumulates linearly with time with a constant event rate density. Let us denote the total number of repeating sources in the universe as N_r and the total event rate of nonrepeating FRBs in the universe as $\dot{N}_n$. One can define a characteristic timescale,

$$T_c \equiv \frac{N_r}{\dot{N}_n}, \quad (6)$$

at which the number of repeating and nonrepeating sources in the sky becomes comparable.[4]

Depending on the effective repeating rate r, a repeating source may be recognized as a repeater (if r is large enough) or an apparent nonrepeater (if r is smaller) or not detected at all (if r is extremely small). We use $f_{\rm rr}$ and $f_{\rm rn}$ to denote the fractions of repeating sources being recognized as repeating and nonrepeating sources, respectively. For nonrepeating sources, only a fraction, $f_{\rm nn}$, are detected with a fluence above $F_{\rm th}$. Therefore, for a sample of observed FRB sources, the fraction of identified repeating sources among all detected sources should be

$$F_{\rm r,obs}(t) = \frac{f_{\rm rr}(t)N_r\frac{\Omega}{4\pi}}{f_{\rm rr}(t)N_r\frac{\Omega}{4\pi} + f_{\rm rn}(t)N_r\frac{\Omega}{4\pi} + f_{\rm nn}\dot{N}_n t\frac{\Omega'}{4\pi}} = \frac{f_{\rm rr}(t)}{f_{\rm rr}(t) + f_{\rm rn}(t) + f_{\rm nn}\frac{t}{T_c}\frac{\Omega'}{\Omega}}, \quad (7)$$

which is a function of the observational time t. Here Ω' is the field of view of the telescope, and Ω is the total sky solid angle the telescope can cover.

2.2. Evolving Repeaters

The evolution of repeaters has two meanings: (1) their intrinsic repeating rates evolve with time, and (2) old sources die and new sources are born all the time in the sky. If the characteristic timescales for these evolution effects are not much longer than the observational timescale, these evolution effects should be considered.

For the repeating rates, we assume that any individual repeater is born with an intrinsic repeating rate $r_0 = r_{0,\rm max}$, which decreases with time as the source ages and finally reaches $r_0 = r_{0,\rm min}$ as the source dies. Assume all of the repeaters have the same lifetime, denoted as T_l. In a steady state, the birth and death rates of the repeating sources would balance each other, so that the total number of sources in the sky would be a constant at any time. But during the observational timescale, N_r would be an accumulated number.

In principle, Equation (7) is still valid under these assumptions, even though the evolution is included. Since a constant parameter is needed to describe the true fraction of repeaters, while T_c, in this case, would be a function of time, we adjust the definition of T_c slightly. Here we use T_c' to represent the modified characteristic timescale, which reads

$$T_c' = \frac{N_{r,0}}{\dot{N}_n} = T_c \times \frac{1}{F}, \quad (8)$$

where $N_{r,0}$ represents the total number of repeating sources at a specific time, and $F = N_r/N_{r,0}$ is a factor for evolution. Consequently, we should also replace $f_{\rm rr}$ and $f_{\rm rn}$ with $f_{\rm rr}' = f_{\rm rr}F$ and $f_{\rm rn}' = f_{\rm rn}F$. Hence, we rewrite Equation (7) as

$$F_{\rm r,obs}(t) = \frac{f_{\rm rr}'(t)}{f_{\rm rr}'(t) + f_{\rm rn}'(t) + f_{\rm nn}\frac{t}{T_c'}\frac{\Omega'}{\Omega}}. \quad (9)$$

When the lifetime of sources is much longer than the observational timescale ($T_l \gg t$), it would reduce to the nonevolving approximation with $F \sim 1$. Hereafter, we only distinguish T_c and T_c' when necessary, but we only use T_c when discussing them together. Similar to the notations T_c and T_c', we do not distinguish between $f_{\rm rr}$ and $f_{\rm rn}$, or between $f_{\rm rr}'$ and $f_{\rm rn}'$ unless it is necessary.

[3] We take a higher minimum energy for nonrepeaters than repeaters. This is because nonrepeaters are supposed to originate from catastrophic events, which likely have higher energies than repeaters in general. For repeaters, the energy of some bursts could, in principle, be below $E_{\rm min}$. For the observational configurations we simulate (similar to that of CHIME), these low-energy bursts are not detectable at cosmological distances.

[4] One may also define $T_c \equiv \rho_r/\dot{\rho}_n$, where ρ_r is the local density of repeating sources and $\dot{\rho}_n$ is the local event rate density of nonrepeating sources. The following discussion remains the same if the redshift distributions of the repeating and nonrepeating sources are roughly the same.

3. Monte Carlo Simulations

In this section, we use Monte Carlo simulations to estimate $f_{\rm rr}$, $f_{\rm rn}$, and $f_{\rm nn}$ and then predict the observed fraction of repeating bursts $F_{\rm r,obs}(t)$ at a certain observational time t. The results depend on several parameters, such as $F_{\rm th}$, T_l, T_c, and r_0. We consider the repeating sources under both the "nonevolving" and "evolving" assumptions separately.

3.1. Nonevolving Repeaters

For nonevolving repeaters, we generate the time sequences of bursts following four steps.

1. Generate a series of repeating sources with a certain redshift distribution.
2. Assign each repeating source an intrinsic repeating rate r_0.
3. Calculate the effective repeating rate for each simulated repeating source.
4. Generate burst time intervals according to the Weibull distribution (given a particular k value) and form a time sequence of the repeated bursts from each repeating FRB source.

In our simulations, we assume that the redshift distributions for both repeating and nonrepeating sources follow the star formation rate (SFR) history. We adopt an analytical fitting formula given by Yüksel et al. (2008),

$$\mathrm{SFR}(z) \propto \left[(1+z)^{3.4\eta} + \left(\frac{1+z}{5000}\right)^{-0.3\eta} + \left(\frac{1+z}{9}\right)^{-3.5\eta}\right]^{1/\eta}, \tag{10}$$

where $\eta = -10$. We generate N_r redshift values according to Equation (10) and assign each value to one repeating FRB source. Choosing appropriate values of $F_{\rm th}$ and r_0 for each repeater, we calculate its effective repeating rate r using Equations (1)–(3).

Assume the observation starts from T_0. A waiting time needs to be introduced to describe how long it takes to detect the first burst from each source. In our simulations, we randomly generate a time interval δ_1 according to Equation (4) and then randomly generate a waiting time t_w in the range of $[0, \delta_1]$.[5] Hence, the first burst appears at $T_1 = T_0 + t_w$. For the sake of convenience, we set $T_0 = 0$. For each repeating source, we simulate N bursts, which appear at $T_i = T_1 + \sum_{j=2}^{i} \delta_j$, where $i = 1, 2, 3 \ldots N$.

3.2. Evolving Repeaters

The main procedure to generate the time sequences of bursts for evolving repeaters follows five steps.

1. Generate a series of repeating sources with a certain redshift distribution.
2. Assign each source an intrinsic repeating rate (r_0) and an age (T_a).
3. Calculate the effective repeating rate for each simulated repeating source.
4. Generate one burst time interval for each repeater according to the Weibull distribution (given a particular k value). Update the intrinsic repeating rate and age.
5. Repeat the previous step until the end of the time sequence exceeds the lifetime of the repeater. Then replace this source with a newly born one.

Under the assumption that the total number of repeaters in the sky at an arbitrary specific time is unchanged because the birth and death rates balance each other, the age of the repeaters (T_a) in the sky should distribute uniformly from zero to their lifetimes. Generate a series of T_a randomly and assign to each source. For each source, every time a burst is produced, we check whether T_i exceeds the lifetime T_l. If so, we record and stop this time sequence and replace it with a new one. Set the new one with the same redshift as the dead one, with $T_a = 0$. The time sequence of the new source's bursts starts from $(T_l - T_{a,i})$. The evolution of r_0 could be introduced when the function of dr_0/dt is given. Update r_0 every time a new time interval is produced.

In principle, we can evolve r_0 and T_a independently. With a similar method as that in Section 3.1, we can obtain a time sequence T_i for each repeater under the evolving assumption.

3.3. Observational Configuration

Since the bursts are simulated with an effective repeating rate r (Equation (3)), all of them are above the flux threshold of a telescope. Those that fall into the field of view of the telescope at the burst time would be detected. In reality, the telescope may not stare at one particular sky area all the time. Therefore, for each repeating source, the observation is not continuous but consists of a number of discrete short-term observations. We assume t_e as the duration of each observation at a certain sky area and t_g as the gap between two observations at the same area. For an observing time t ($t < T_{i=N}$) for a telescope, there are $n = t/(t_e + t_g)$ observing periods. From a simulation, we count the number of T_i for each source that satisfy $m(t_e + t_g) < T_i < t_e + m(t_e + t_g)$, where $m = 0, 1, 2 \ldots n - 1$. If more than one burst was detected, it would be recognized as a repeater; if exactly one burst was detected, it would be recognized as an apparently nonrepeating source; otherwise, the source would not be detected. Investigating all of the sources in the simulation, we can obtain the values of $f_{\rm rr}$ and $f_{\rm rn}$.

Nonrepeating sources are generated following the redshift (Equation (10)) and energy (Equation (5)) distributions. The fraction $f_{\rm nn}$ could be estimated through dividing the number of detectable nonrepeating bursts by the total number of simulated nonrepeating sources. Note that $f_{\rm nn}$ is not a function of time.

In our simulations, we take the threshold fluence as $F_{\rm th} = 4$ Jy ms, which is comparable to CHIME's sensitivity (CHIME/FRB Collaboration et al. 2019b; Fonseca et al. 2020). We generate 10^6 nonrepeating sources with $E_{\rm n,min} < E < E_{\rm n,man}$, so that $f_{\rm nn}$ can be determined as $\sim$0.0035. According to our definition, the total solid angle Ω covered by the telescope would be observed once in $t_e + t_g$, and t_e is the effective observational time for the field of view with a solid angle Ω'. We then have $\Omega'/\Omega = nt_e/t$. Equations (7) and (9) can then be rewritten as

$$F_{\rm r,obs} = \frac{f_{\rm rr}(t)}{f_{\rm rr}(t) + f_{\rm rn}(t) + f_{\rm nn}\frac{nt_e}{T_c}} \tag{11}$$

[5] When $k = 1$ in Equation (4) is assumed, the distribution of t_w is the same as that of δ.

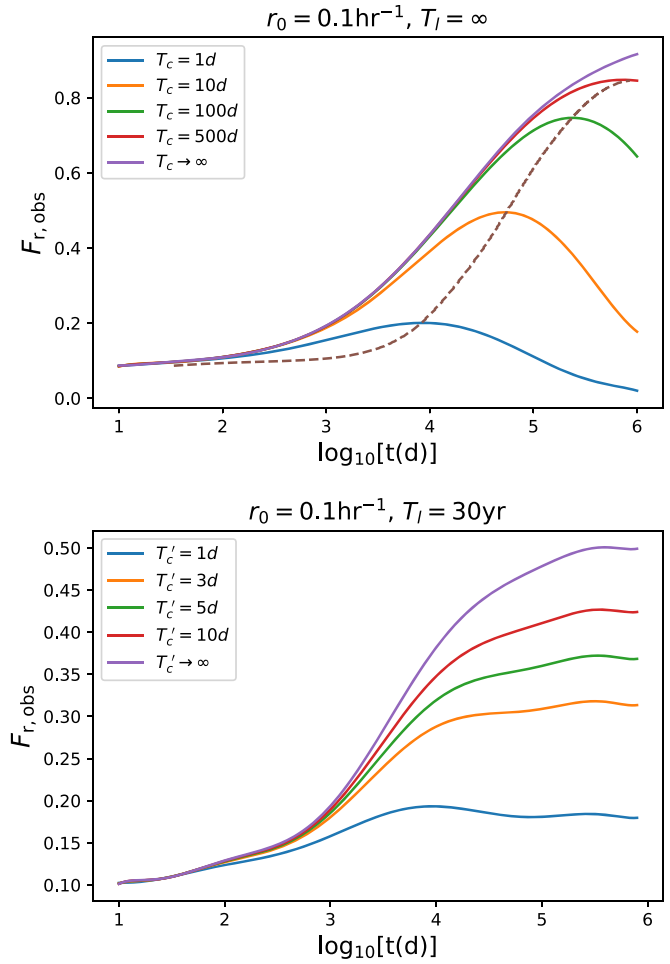

Figure 1. Observed repeater fraction $F_{\mathrm{r,obs}}$ as a function of time. The colored solid lines delineate the evolution of $F_{\mathrm{r,obs}}$ for different T_c values. Upper panel: constant repeating rate ($r_0 = 0.1\ \mathrm{hr}^{-1}$) with infinity lifetime. The dashed line marks the trajectory of the peak fraction vs. peak time as a function of T_c. Lower panel: constant repeating rate ($r_0 = 0.1\ \mathrm{hr}^{-1}$) with lifetime $T_l = 30\mathrm{yr}$. The following parameters are adopted for both panels: $t = n(t_e + t_g)$, where $t_e = 0.2$ hr and $t_g = 23.8$ hr; the Weibull parameter is adopted as $k = 0.3$ (Oppermann et al. 2018).

and

$$F_{\mathrm{r,obs}} = \frac{f'_{\mathrm{rr}}(t)}{f'_{\mathrm{rr}}(t) + f'_{\mathrm{rn}}(t) + f_{\mathrm{nn}}\frac{nt_e}{T_c}}. \quad (12)$$

4. Results

4.1. Evolution of $\mathrm{F}_{r,obs}$

Our first goal is to investigate how the observed repeater fraction, $F_{\mathrm{r,obs}}$, evolves with time and how this evolution depends on the parameter T_c, a characteristic parameter to define the relative fractions between the genuine repeaters and nonrepeaters: $T_c \to \infty$ means that all FRBs are repeaters, and $T_c \to 0$ means that the majority of FRBs are genuine nonrepeaters.

4.1.1. Nonevolving Repeaters

We first give an example by assuming that all repeaters are as active as the first repeating source, FRB 121102 ($r_0 = 0.1$ hr^{-1} (Law et al. 2017; James 2019), and last forever. The observed fraction of repeating sources $F_{\mathrm{r,obs}}$ as a function of observational time t is shown in the upper panel of Figure 1. For $T_c \to \infty$, $F_{\mathrm{r,obs}}$ always increases, but the slope decreases as a function of time. If T_c is a finite value, which means that there are genuine nonrepeating sources, $F_{\mathrm{r,obs}}$ increases with time first because of the fast increase of f_{rr} in the beginning. Later on, the increase of f_{rr} slows down because one already recognizes most of the repeaters. On the other hand, the number of nonrepeating sources linearly increases with time, so that $F_{\mathrm{r,obs}}$ reaches a peak and then starts to decline afterward.

In the following, we denote the expected maximum fraction of repeating sources as the "peak fraction" ($F_{\mathrm{r,obs,p}}$), and its corresponding time is expressed as the "peak time" (T_p).

From the upper panel of Figure 1, we can see that the distinction of $F_{\mathrm{r,obs}}$ curves for different T_c is insignificant when t is short. A distinct feature occurs around the peak time. The peak time and fraction are the most crucial observational quantities that can be used to estimate T_c. A smaller T_c corresponds to a more dominant nonrepeater population, which corresponds to a smaller peak time and a lower peak fraction.

4.1.2. Evolving Repeaters

Keep $r_0 = 0.1\ \mathrm{hr}^{-1}$ and set a finite lifetime as $T_l = 30$ yr for all repeaters. The evolution of $F_{\mathrm{r,obs}}$ is shown in the lower panel. The curves flatten when $t \gg 30$ yr. Because the observational timescale can totally cover the entire lifetime of the repeaters, both repeating and nonrepeating bursts would accumulate linearly with time with constant rates. Therefore, $F_{\mathrm{r,obs}}$ may never approach 1 but rather balance at a certain level smaller than 1, even if $T_c' \to \infty$. If T_c' is small, a peak of $F_{\mathrm{r,obs}}$ could be observed at $T_p < T_l$. Hence, with a large T_l, a peak would still be expected. See the lower panel of Figure 1.

4.2. Effect of Key Parameters

As already known from Section 4.1, with a fixed r_0, T_c is a parameter that strongly influences T_p and $F_{\mathrm{r,obs,p}}$. In this section, we allow the value of r_0 to vary among repeating FRBs to get more realistic results.

4.2.1. Nonevolving Repeaters

Our simulation starts from nonevolving repeaters. The evolution of r_0 and the birth and death of sources are not included. We consider that the values r_0 for different sources follow a power-law distribution, i.e.,

$$\frac{dn^*}{dr_0} \propto r_0^{-q}, \quad (13)$$

where dn^* represents the number of repeating sources with the intrinsic repeating rate in the range of $r_0 \sim r_0 + dr_0$. For this distribution, one can introduce three parameters: two for the r_0 range ($r_{0,\mathrm{min}}$ and $r_{0,\mathrm{max}}$) and one for the power-law index (q). Among these three parameters, $r_{0,\mathrm{max}}$ is the most accessible one, which could be directly measured from the most active repeating sources in the universe (e.g., active repeaters at a relatively large distance). The index q can also be obtained observationally by fitting the repeaters' repetition rate distribution. However, the value of $r_{\mathrm{min},0}$ is much more difficult to determine, because observationally, it is hard to distinguish a repeating source with a very low r_0 from an intrinsically nonrepeating burst.

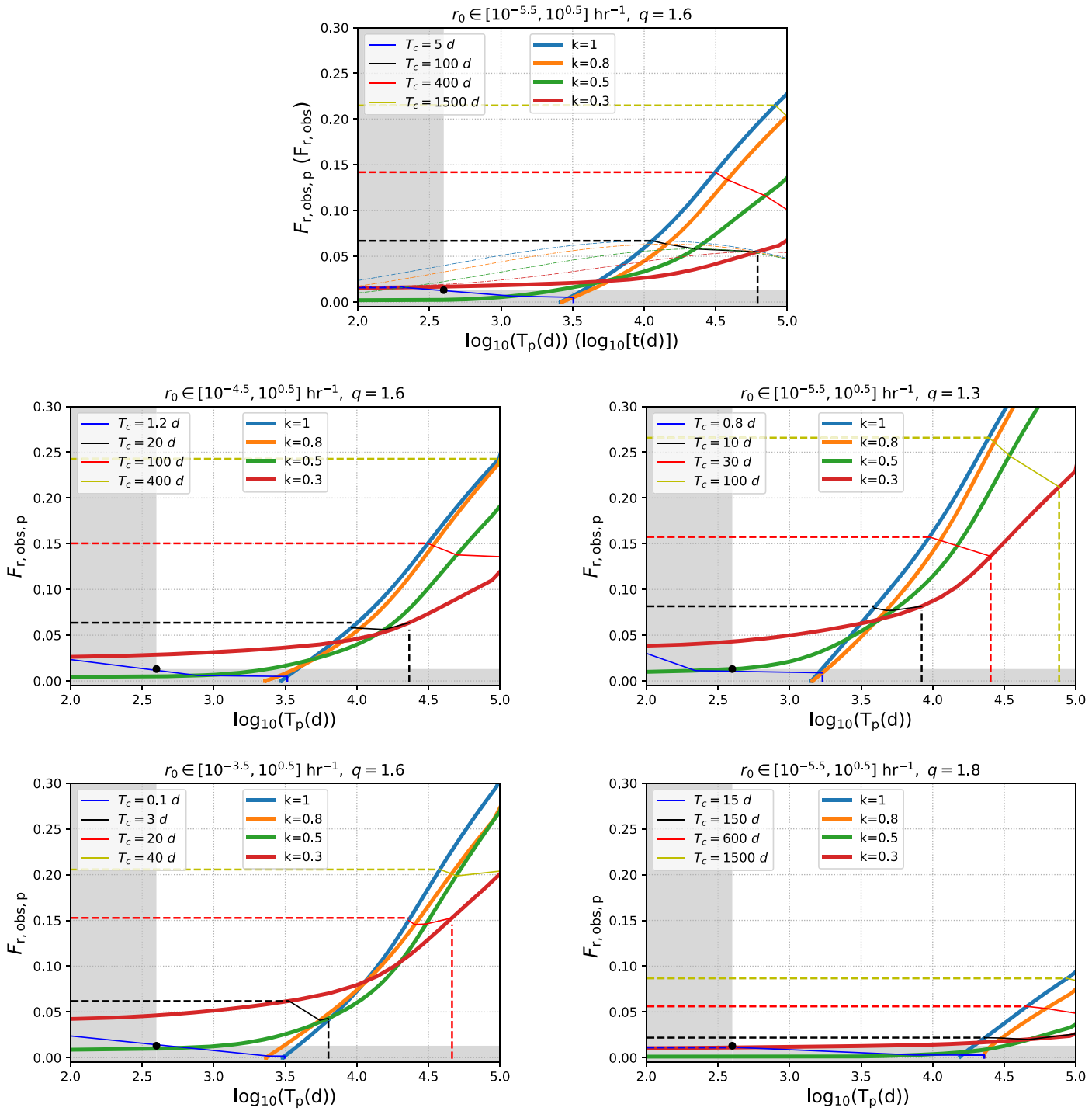

Figure 2. Observed peak repeater fraction and peak time ($T_p - F_{\rm r,obs,p}$) of repeating FRB sources for different model parameters under the "nonevolving repeater" assumption. All panels allow an r_0 distribution among repeating FRB sources, with different r_0 distribution range and q values marked on top of each panel. Solid lines stand for the locus (T_p, $F_{\rm r,obs,p}$) when different T_c (thin solid colored lines) and k (thick solid colored lines) values are assumed. Dashed lines are the most conservative constraints on T_c through the observational time t and observed fraction $F_{\rm r,obs}$ before a peak is reached. In the upper panel, the dotted–dashed lines show the evolution of $F_{\rm r,obs}$ as a function of time as examples. The black dot in each panel stands for the observational time and fraction of repeating sources according to the CHIME 400-d observation results (Fonseca et al. 2020). All five figures make the assumption of $t = n(t_e + t_g)$, where $t_e = 0.2$ and $t_g = 23.8$ hr.

In our simulation, we adopt a fixed maximum repeating rate $r_{0,\rm max} = 10^{0.5}{\rm hr}^{-1}$, which is obtained by fitting CHIME's latest repeating FRB sample (Lu et al. 2020). We then choose different $r_{0,\rm min}$ and q values to see how they influence the simulation results. We fix one of these two parameters and vary the other one in every simulation. The results are shown in Figure 2 with solid lines denoting the locus of (T_p, $F_{\rm r,obs,p}$) as the parameters are varied. When we set a fixed index as $q = 1.6$ and vary the value of $r_{0,\rm min}$, the results are shown in the middle-left and bottom-left panels of Figure 2. With the same T_c, a lower $r_{0,\rm min}$ would lead to a smaller $F_{\rm r,obs,p}$ and T_p. When we set $r_{0,\rm min} = 10^{-5.5}\,{\rm hr}^{-1}$ and vary the value of q, the results are shown in the middle-right and bottom-right panels of

Figure 2. With the same T_c, a higher q would lead to a smaller $F_{\rm r,obs,p}$ and T_p.

Both a lower $r_{0,\rm min}$ and a higher q would make more repeating sources with low r_0 values. Consider that the increase of $f_{\rm rr}$ slows down when most of the sources that repeat frequently enough have been recognized as repeating sources. If there are more low r_0 sources, $f_{\rm rr}$ would have a smaller absolute value, and its increase rate would become smaller. This explains why both $F_{\rm r,obs,p}$ and T_p become smaller in these cases.

4.2.2. Evolving Repeaters

In this section, we set r_0 and T_a to have a one-to-one correspondence. As assumed above, the birth and death of repeaters balance each other, which means that their age distribution is stable; thus, the r_0 distribution should also be stable. We then assume that all of the repeaters are born with $r_0 = r_{0,\rm max}$ and die with $r_0 = r_{0,\rm min}$ with the same evolutionary track, which can be derived from the r_0 distribution at an arbitrary time.

Using the power-law distribution in Equation (13), T_a changes with r_0 as

$$\frac{dT_a}{dr_0} = \frac{T_l(-q+1)}{r_{0,\rm max}^{-q+1} - r_{0,\rm min}^{-q+1}} r_0^{-q}, \tag{14}$$

where T_l is the lifetime of the sources. Hence, the age of a repeater could be estimated from its intrinsic repeating rate as

$$T_a = \frac{r_{0,\rm max}^{-q+1} - r_0^{-q+1}}{r_{0,\rm max}^{-q+1} - r_{0,\rm min}^{-q+1}} T_l. \tag{15}$$

The evolution of r_0 follows

$$\frac{dr_0}{dt} = \frac{r_{0,\rm max}^{-q+1} - r_{0,\rm min}^{-q+1}}{T_l(-q+1)} r_0^q. \tag{16}$$

Considering both the lifetime and evolution of the intrinsic repeating rate, we conduct simulations with the same parameter sets used in Section 4.2.1. We find that T_c', $r_{0,\rm min}$, and q influence $F_{\rm r,obs,p}$ and T_p with the same trend as that with nonevolving repeaters, which is shown in Figure 3. For the same (T_p, $F_{\rm obs,p}$) pair, the required T_c' is slightly greater than T_c. This is understandable because the repeating rate decreases with time under the evolving assumption, which would lead to fewer repeating sources to be recognized; hence, fewer genuine nonrepeating sources are expected. However, the difference is insignificant because the lifetime of repeaters is assumed to be much longer than the observational timescale.

In Figures 2 and 3, we also allow the shape parameter k for the Weibull distribution to vary in different simulations. We find that the k value would dramatically influence the peak time but only slightly influence the peak fraction when other parameters are set to fixed values.

4.3. Constraints on $\rm T_c$

Four parameters (T_c, $r_{0,\rm min}$, q, and k) have been discussed in the previous sections. The latter three parameters are related to repeating sources only, which may eventually be measured from the observations of repeaters. The T_c parameter concerns the true relative fractions of repeaters and nonrepeaters, which cannot be measured directly from the repeater data only. It may, however, be constrained from the observed $F_{\rm r,obs}$ as a function of time or the measurement of $(T_p - F_{\rm r,obs,p})$ if a peak indeed exists. In principle, for a reasonable k range (e.g., from 0.3 to 1), once a peak is detected, one may find an appropriate r_0 distribution to make the observed peak point located in the region of the predicted peak points within the assumed k range (contours in Figures 2 and 3). Finding the T_c contour line that goes through the observed peak point, one can then determine both T_c and k. In reality, there might not be only one r_0 distribution that can satisfy the observational constraint. Hence, constraints on the r_0 distribution from the repeating FRB data would be helpful to make more stringent constraints on T_c.

According to our simulations, depending on parameters T_p can be much longer than the observational timescale, e.g., up to thousands of years. In general, even when the peak (if it exists), i.e., (T_p, $F_{\rm r,obs,p}$), has not been detected yet, one can still put constraints on T_c. Similar to the case with an observed peak, one can also find the T_c value corresponding to the current $F_{\rm r,obs}$ and observational time t. This T_c value would serve as the lower limit, since both $F_{\rm r,obs,p}$ and T_p increase with T_c. In the case when $F_{\rm r,obs}$ and t do not appear in the solid T_c contour region in Figures 2 and 3, we also plot the conservative constraints on T_c with dashed lines in Figures 2 and 3. The observational run by CHIME from 2018 August 28 to 2019 September 30 detected ~700 new FRBs with nine repeaters (Fonseca et al. 2020). We thus place the fraction 0.013 with 400 days of observation in each panel of Figures 2 and 3 to denote the current data constraint.

The simulated evolution curve of $F_{\rm r,obs}$ should certainly pass through the observational value. Once the predicted $F_{\rm r,obs}$ is lower than the observed value even when $T_c \to \infty$, this parameter set of repeaters should be ruled out. If the predicted $F_{\rm r,obs}$ is higher than the truly observed value, one can still lower the T_c value to meet the data constraint. Hence, under the assumption that r_0 satisfies a power-law distribution, since a lower $r_{0,\rm min}$ leads to a lower $f_{\rm rr}$ and thus a lower predicted $F_{\rm r,obs}$, the current data point could place a lower limit on $r_{0,\rm min}$. As shown in the upper panel of Figure 4, for $k = 0.3$ (the favored value of k for FRB 121102; Oppermann et al. 2018), $r_0 < 10^{-6.5}$ hr would be disfavored, since the evolution of $F_{\rm r,obs}$ would never pass through the current data point. However, if we relax the constraints on k, $r_{0,\rm min} < 10^{-6.5}$ hr would still be possible. For $k = 1$, $r_{0,\rm min}$ could be as low as $10^{-10.5}\,\rm hr^{-1}$ without violating the current data point. If $r_{0,\rm min} = 10^{-14}$ hr, which corresponds to the Hubble timescale, is chosen, the evolving curve of the observed fraction of repeating FRBs would remain near zero all the time, because repeating FRBs in this case are extremely hard to detect. This figure is made under the "nonevolving" assumption. If evolution is considered, as discussed in Section 4.2.2, the results will be very similar. Hereafter, we will not discuss "evolving" and "nonevolving" cases separately, because when the distribution of r_0 is considered, their results are very close. We also test other q values from 1 to 2.[6] It turns out that the general trend does not change, with the results slightly differing in numbers. This is reasonable because both $f_{\rm rr}$ and $f_{\rm rn}$ would

[6] If $q > 2$, most of the repeaters are located at the lower end of the r_0 distribution, which makes it extremely difficult to observe a burst produced from them. It is even more difficult to detect them as repeaters. This means that the observed $F_{\rm r,obs}$ would remain very small for a long time; thus, it would be inefficient to pose a lower limit on T_c. However, a large q value is already disfavored by the current date because it would not lead to an $F_{\rm r,obs}$ value as large as 0.013. In the following, we do not consider the case with $q > 2$.

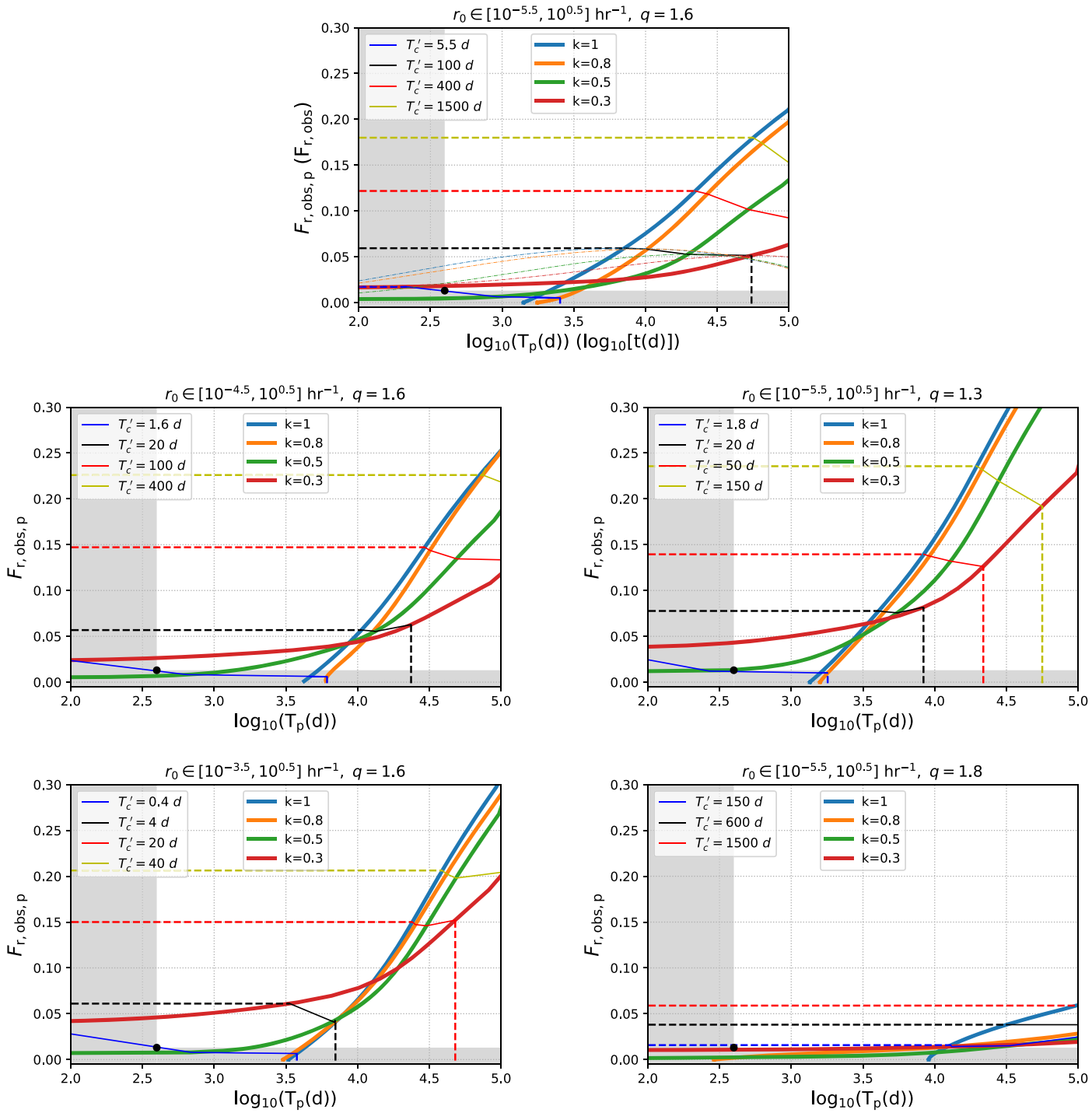

Figure 3. Observed peak repeater fraction and peak time of repeating FRB sources under the "evolving repeater" assumption. All notations are the same as those of Figure 2.

decrease with a lower $r_{0,\min}$ or larger q. Thus, the decrease of $F_{r,obs}$ would not be very significant.

On the other hand, with a certain r_0 distribution and a reasonable range of k assumed, one can put both upper and lower limits on T_c. Compared with the lower limit obtained from the peak fraction constraint discussed above, the lower limit of T_c here would be more conservative, because here we do not involve the assumption that the observed fraction of repeaters has not yet reached the peak value.

Considering that the current CHIME data point of the observed fraction of repeaters is relatively low, we have reason to expect a higher $F_{r,obs}$ with a longer observational timescale in the future. Even if the current data point has passed the peak fraction, the current observed fraction should still be around the peak value. Hence, we adopt the lower limit obtained from Figures 2 and 3 while using the evolution curve of $F_{r,obs}$ to get its upper limit, as shown in the lower panel of Figure 4.

In Table 1, we summarize the constraints on T_c with the CHIME data point t and $F_{r,obs}$ values for the assumed range of

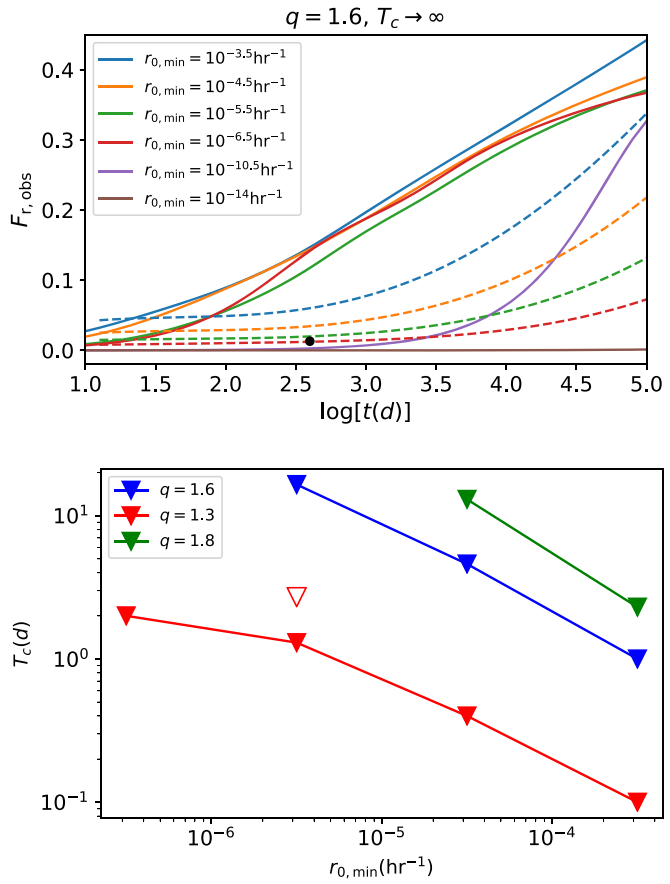

Figure 4. Upper panel: evolution of $F_{\mathrm{r,obs}}$ with different $r_{0,\min}$ values adopted. The black dot is the same as that in Figure 2, which represent the current data point. The solid and dashed lines stand for the cases for $k = 1$ and 0.3, respectively. Lower panel: upper limit of T_c with the current observed fraction of repeaters. The minimum value of r_0 serves as the horizontal axis, while the results with different q values are shown with different colors. The solid triangles and lines stand for the nonevolving repeater case, while the hollow triangle stands for the evolving repeater case. The upper limits are obtained with $k = 0.3$–1.

k. For each parameter set, combining the lower and upper limits together, one can constrain T_c to a small range. However, since some parameters of the repeaters' population have not yet been determined, the range of the possible T_c would be very large, which is 0.1 day $< T_c < \infty$. Considering those constraints on T_c, we could predict the observed fraction of repeaters in the future with a CHIME-like telescope array, with a duty cycle as assumed in this paper. Our predictions are shown in Table 2. The bold font represents the cases in which the peak should have appeared, whereas the regular font represents the cases in which the peak may not have appeared yet. We find that for all of the parameter sets, there would not be a significant increase of $F_{\mathrm{r,obs}}$ with 3, 10, or even 30 yr observations. In most cases, the peak would be observed in 30 yr. The peak fraction of repeaters would not be more than 0.04 in all cases.

5. Conclusions and Discussion

We have introduced a parameter T_c (T_c' for evolving repeaters; defined in Equation (6), or Equation (8) for the evolving case) to describe the real fraction of repeating FRB sources in the entire universe. A smaller T_c means a larger fraction of genuinely nonrepeating sources per unit time. The ansatz that all FRBs repeat corresponds to $T_c \to \infty$. Considering that not all repeating sources can be recognized, we performed a set of Monte Carlo simulations to investigate how the observed repeating source fraction $F_{\mathrm{r,obs}}$ is related to the true fraction (T_c as a proxy).

Assuming that all repeaters have the same intrinsic repeating rate, we found the following.

1. If all repeaters are nonevolving, once a finite T_c is introduced, $F_{\mathrm{r,obs}}$ will not always increase with time but instead shows a turnover after reaching a peak value $F_{\mathrm{r,obs,p}}$ at a peak time T_p. The expected turnover point is highly dependent on T_c, with a larger T_c corresponding to a higher $F_{\mathrm{r,obs,p}}$ and later T_p.
2. If the evolution of repeaters is considered, a turnover point is expected only if T_p is smaller than their characteristic lifetime T_l. When the observational timescale is longer than T_l, $F_{\mathrm{r,obs}}$ would roughly be a constant. The curve of $F_{\mathrm{r,obs}}$ would be flattened even if $T_c' \to \infty$.

The (T_p, $F_{\mathrm{r,obs,p}}$) pair also depends on the repeating rate distribution of the repeaters, as well as the time distribution function of the bursts (the Weibull parameter k). Assume the intrinsic repeating rate r_0 satisfies a power-law distribution with an index q in the range of [$r_{0,\mathrm{rmin}}$, $r_{0,\mathrm{rmax}}$] and fix $r_{0,\max}$ (which could be measured from known repeaters). We found the following.

1. In the nonevolving repeater approximation, a higher q and lower $r_{0,\min}$ would both result in a distribution with more inactive repeating sources, which would lead to a lower $F_{\mathrm{r,obs,p}}$ and an earlier T_p. With other parameters fixed, the k parameter would dramatically influence T_p but only slightly change $F_{\mathrm{r,obs,p}}$.
2. Assume that the distribution of r_0 at a specific time is introduced by the evolution of r_0 with time and that the lifetime of the repeaters is longer than the observational timescale. The trend of how different parameters influence T_p and $F_{\mathrm{r,obs,p}}$ remains the same as that in the nonevolving approximation case.

Available CHIME observations give $F_{\mathrm{r,obs}} \sim 0.013$ at $t \sim 400$ days. One may regard this as a lower limit of $F_{\mathrm{r,obs,p}}$ and T_p, so that the data can already place a lower limit on T_c, i.e., $T_c > 0.1$ days with reasonable parameters. In the future, if a higher value of $F_{\mathrm{r,obs}}$ is observed, a more stringent lower limit on T_c can be obtained. The theoretical evolution curve of $F_{\mathrm{r,obs}}$ should always pass through the current data point; thus, an upper limit on T_c could also be obtained, albeit with a large uncertainty. We predict that the observed fraction of repeaters would remain smaller than 0.04 with 30 yr observations with CHIME or similar telescope arrays. If a peak fraction smaller than 0.04 is actually observed in the near future, the ansatz that all FRB sources repeat would be disfavored.

All conclusions drawn in this paper are based on the assumption that all of the repeaters have the same r_0 or that the r_0 follows a power-law distribution. So far, there is no direct measurement of the r_0 distribution. However, such a distribution can be readily measured when more repeating FRBs are closely monitored. If in the future, the r_0 distribution is proven not to be a power law, some of our conclusions need to be reinvestigated.

S.A. and B.Z. acknowledge the Top Tier Doctoral Graduate Research Assistantship (TTDGRA) at University of Nevada,

Table 1
Constraints on T_c with Current Data

$q\backslash r_{0,\min}$ (hr^{-1})	$10^{-3.5}$	$10^{-4.5}$	$10^{-5.5}$	$10^{-6.5}$	$10^{-10.5}$
1.3	$T_c < 0.1$ d	$T_c < 0.4$ d	0.8 d $< T_c <$ 1.3 d	$T_c < 2.0$ d	$T_c < 35$ d
1.6	0.1 d $< T_c <$ 1.0 d	1.2 d $< T_c <$ 4.6 d	5 d $< T_c <$ 16.5 d	15 d $< T_c < \infty$	$T_c \to \infty$
1.8	$T_c < 2.3$ d	$T_c < 13$ d	15 d $< T_c < \infty$	3000 d $< T_c < \infty$	⋯

Las Vegas, for support. H.G. acknowledges the National Natural Science Foundation of China (NSFC) under grant Nos. 11722324 and 11690024 and the Fundamental Research Funds for the Central Universities for support. B.Z. thanks Xuelei Chen for a stimulating conversation.

Appendix
Weibull Distribution

The distribution of the time interval of two adjacent bursts in a repeating source could be described by a Weibull function, which reads

$$\mathcal{W}(\delta|k, r) = k\delta^{-1}[\delta r\Gamma(1 + 1/k)]^k e^{-[\delta r\Gamma(1+1/k)]^k}, \quad \text{(A1)}$$

where r represents the mean repeating rate, k is the shape parameter, and $\Gamma(x)$ stands for the gamma function.

When $k = 1$, the distribution is reduced to the exponential (i.e., Poisson) distribution. In this case, Equation (A1) is simplified as

$$\mathcal{W}(\delta|r) = re^{-r\delta}. \quad \text{(A2)}$$

The mean interval time is

$$\langle\delta\rangle = \int_0^\infty \delta\mathcal{W}(\delta|r)d\delta = 1/r. \quad \text{(A3)}$$

The variance of δ could be calculated as

$$\begin{aligned} D(\delta) &= \langle\delta^2\rangle - \langle\delta\rangle^2 \\ &= \int_0^\infty \delta^2\mathcal{W}(\delta|r)d\delta - \frac{1}{r^2} \\ &= \frac{2}{r^2} - \frac{1}{r^2} \\ &= \frac{1}{r^2}. \end{aligned} \quad \text{(A4)}$$

Assume that an observation starts at time t_s after the first burst, and the waiting time until the next burst appears is t_w. The probability that an observer would wait for at least a period of t_1 could be written as

$$\begin{aligned} P(t_w > t_1) = P(\delta > t_s + t_1|\delta > t_s) &= \frac{e^{-r(t_1+t_s)}}{e^{-rt_s}} \\ &= e^{-rt_1}. \end{aligned} \quad \text{(A5)}$$

Similarly, the probability of having a burst in t_1 would be

$$P(t_w < t_1) = 1 - e^{-rt_1}, \quad \text{(A6)}$$

which is independent of t_s. The probability density function is

$$\mathcal{W}(t_w|r) = re^{-rt_w}, \quad \text{(A7)}$$

which is the same as that of the time interval δ. Therefore, the mean waiting time is the same as the true mean interval time between two adjacent bursts.

When $k \neq 1$, one can similarly calculate the mean time interval as

$$\begin{aligned} \langle\delta\rangle &= \int_0^\infty \delta\mathcal{W}(\delta|r)d\delta \\ &= \int_0^\infty k[\delta r\Gamma(1 + 1/k)]^k e^{-[\delta r\Gamma(1+1/k)]^k}d\delta \\ &= \frac{1}{r\Gamma(1 + 1/k)}\int_0^\infty x^{1/k}e^{-x}dx, \end{aligned} \quad \text{(A8)}$$

where $x = [\delta r\Gamma(1 + 1/k)]^k$. Considering that $\Gamma(1 + z) = \int_0^\infty x^z e^{-x}dx$, one has

$$\langle\delta\rangle = \frac{1}{r\Gamma(1 + 1/k)} \times \Gamma(1 + 1/k) = \frac{1}{r}. \quad \text{(A9)}$$

The mean time interval does not change with k.

We can calculate the variance of the Weibull distribution to study the clustering effect introduced by the shape parameter k. The variance is

$$\begin{aligned} D(\delta) &= \langle\delta^2\rangle - \langle\delta\rangle^2 \\ &= \int_0^\infty \delta^2\mathcal{W}(\delta|r)d\delta - \frac{1}{r^2} \\ &= \frac{1}{[r\Gamma(1 + 1/k)]^2}\int_0^\infty x^{2/k}e^{-x}dx - \frac{1}{r^2} \\ &= \frac{1}{r^2}\left[\frac{\Gamma(1 + 2/k)}{\Gamma(1 + 1/k)^2} - 1\right]. \end{aligned} \quad \text{(A10)}$$

Compared with exponential distribution, the variance of the Weibull distribution is corrected by a factor of

$$f(k) = \frac{\Gamma(1 + 2/k)}{\Gamma(1 + 1/k)^2} - 1 \quad \text{(A11)}$$

as a function of k, which is shown in Figure 5.

When $k < 1$, the variance of the Weibull distribution is larger than $1/r^2$, which means that both longer and shorter time intervals have more chances to appear. That would lead to the case that some bursts are closer to each other, and some others are more separated from each other. Hence, we tend to detect "clusters" of bursts. When $k > 1$, the variance of the Weibull distribution would be smaller than $1/r^2$, which means that the time intervals between bursts tend to be the same. In this case, the repeating burst would appear to be more "periodic."

In addition, when $k \neq 1$, the waiting time distribution is not the same as the time interval distribution.

ORCID iDs

Shunke Ai https://orcid.org/0000-0002-9165-8312
He Gao https://orcid.org/0000-0002-3100-6558
Bing Zhang https://orcid.org/0000-0002-9725-2524

Table 2
Predictions for Future Observations

$t\backslash r_0$	$r_{0,\min} = 10^{-3.5}$ $q = 1.6$	$r_{0,\min} = 10^{-4.5}$ $q = 1.6$	$r_{0,\min} = 10^{-5.5}$		
			$q = 1.3$	$q = 1.6$	$q = 1.8$
3 yr	$F_{\rm r,obs} < 0.04$	$F_{\rm r,obs} < 0.03$	$F_{\rm r,obs} < 0.02$	$F_{\rm r,obs} < 0.02$	$F_{\rm r,obs} < 0.013$
10 yr	$F_{\rm r,obs} < 0.04$	$F_{\rm r,obs} < 0.03$	$\boldsymbol{F}_{\rm r,obs,p} < 0.04$	$\boldsymbol{F}_{\rm r,obs,p} < 0.02$	$F_{\rm r,obs} < 0.013$
30 yr	$\boldsymbol{F}_{\rm r,obs,p} < 0.04$	$\boldsymbol{F}_{\rm r,obs,p} < 0.03$	$\boldsymbol{F}_{\rm r,obs,p} < 0.04$	$\boldsymbol{F}_{\rm r,obs,p} < 0.02$	$F_{\rm r,obs} < 0.015$

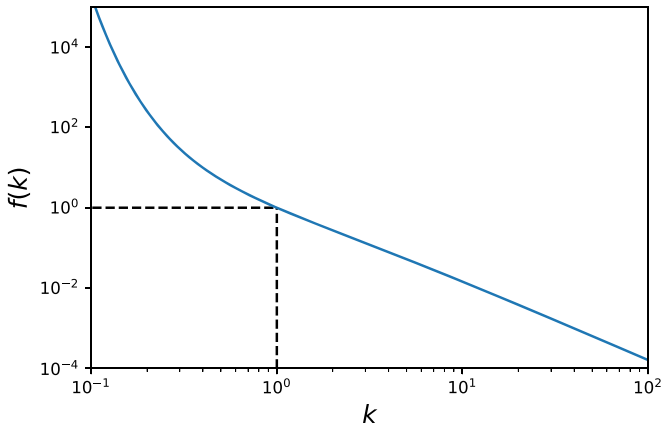

Figure 5. Correcting factor $f(k)$ of the variance of the Weibull distribution compared with the exponential distribution as a function of shape parameter k.

References

Bochenek, C. D., Ravi, V., Belov, K. V., et al. 2020, Natur, 587, 59
Caleb, M., Stappers, B. W., Rajwade, K., & Flynn, C. 2019, MNRAS, 484, 5500
CHIME/FRB Collaboration, Amiri, M., Bandura, K., et al. 2019a, Natur, 566, 235
CHIME/FRB Collaboration, Andersen, B. C., Bandura, K., et al. 2019b, ApJL, 885, L24
Cordes, J. M., & Chatterjee, S. 2019, ARA&A, 57, 417
Fonseca, E., Andersen, B. C., Bhardwaj, M., et al. 2020, ApJL, 891, L6
James, C. W. 2019, MNRAS, 486, 5934
Law, C. J., Abruzzo, M. W., Bassa, C. G., et al. 2017, ApJ, 850, 76
Lorimer, D. R., Bailes, M., McLaughlin, M. A., Narkevic, D. J., & Crawford, F. 2007, Sci, 318, 777
Lu, W., & Piro, A. L. 2019, ApJ, 883, 40
Lu, W., Piro, A. L., & Waxman, E. 2020, MNRAS, 498, 1973
Luo, R., Lee, K., Lorimer, D. R., & Zhang, B. 2018, MNRAS, 481, 2320
Luo, R., Men, Y., Lee, K., et al. 2020, MNRAS, 494, 665
Oppermann, N., Yu, H.-R., & Pen, U.-L. 2018, MNRAS, 475, 5109
Palaniswamy, D., Li, Y., & Zhang, B. 2018, ApJL, 854, L12
Petroff, E., Hessels, J. W. T., & Lorimer, D. R. 2019, A&ARv, 27, 4
Petroff, E., Johnston, S., Keane, E. F., et al. 2015, MNRAS, 454, 457
Ravi, V. 2019, NatAs, 3, 928
Spitler, L. G., Scholz, P., Hessels, J. W. T., et al. 2016, Natur, 531, 202
The CHIME/FRB Collaboration, Andersen, B. C., et al. 2020, Natur, 587, 54
Thornton, D., Stappers, B., Bailes, M., et al. 2013, Sci, 341, 53
Yüksel, H., Kistler, M. D., Beacom, J. F., & Hopkins, A. M. 2008, ApJL, 683, L5